COBEM 2021 26th International Congress of Mechanical Engineering
ABCM Associação Brasileira de Engenharia e Ciências Mecânicas
November 22-26, 2021, Virtual Congress, Brazil

COB-2021-1542
PERFORMANCE ANALYSIS OF OSCILLATING HYDROFOILS WITH DIFFERENT WING PROFILES

Guilherme Amaral do Prado Campos[1,2]
Luciano Santos Constantin Raptopoulos[3]
Max Suell Dutra[1]

[1]Mechanical Engineering Department, Federal University of Rio de Janeiro, 2030 Horácio Macedo Av., Technology Center, Cidade Universitária, Rio de Janeiro, RJ, 21941-914, Brazil

[2]Mechanical Engineering Department, Federal Center for Technological Education Celso Suckow da Fonseca, 1317 Adrianópolis Road, Nova Iguaçu, RJ, CEP 26041-271, Brazil

[3]Control and Automation Engineering Department, Federal Center for Technological Education Celso Suckow da Fonseca, 1317 Adrianópolis Road, Nova Iguaçu, RJ, CEP 26041-271, Brazil

guilherme.campos@cefet-rj.br, luciano.raptopoulos@cefet-rj.br and max@mecanica.coppe.ufrj.br

Abstract. *The different energy converters employed in the ocean seek continuous improvement to make their operation in the world electrical matrix viable. The flapping foil is among the evolving models, which uses tidal or ocean currents to generate electrical energy. This device is inspired by the fish fins and has a harmonic motion, similar to sea life, promoting a friendly interaction with the environment. The present work developed a mathematical model validated with experiments in the literature, considering such aspects as mass and added damping, thrust, and variation of the angle of attack along the operation cycle. In the model simulations, the three symmetrical NACA profiles most used in the literature (NACA 0012, NACA 0014, and NACA 0015) were evaluated under different operating conditions, with the number of Reynolds (Re) ranging from* 1.5×10^5 *to* 5.0×10^5*. In addition, some parameters were considered constant, such as chord; arm; span; pitch and heave amplitude; maximum limit of the angle of attack (due to the restrictions of the data collected via the XFOIL algorithm, which was implemented in the modeling). This algorithm, XFOIL, generates the hydrodynamic forces of the profiles according to the number of Mach, Re and angle of attack, based on the panel method and the boundary layer theory. Therefore, this algorithm has restrictions after the hydrodynamic profile reaches the stall. Thus, limits of the angle of attack were adopted, and the model was validated with the literature. The mathematical modeling showed satisfactory results, and the simulations between the adopted symmetrical NACA profiles demonstrated gains when choosing the most appropriate model. Finally, it was found that the NACA 0015 profile is the most suitable for the Reynolds number, equal to* 2.5×10^5 *and* 5.0×10^5 *when compared to the others. In the case of Re =* 1.5×10^5*, NACA 0014 and NACA 0015 have a similar performance.*

Keywords: *flapping foil, oscillating hydrofoil, tidal energy, dynamic model, symmetrical NACA*

1. INTRODUCTION

The generation of energy in the world is a topic under constant discussion. The use or not of fossil fuels is addressed at all climate summits and the use of renewable energy to replace such a source. The growth of renewable sources has stimulated world powers, and Brazil has been following these changes. When comparing the Brazilian electricity matrix of the last decade, there was a diversification of renewable sources, no longer relying exclusively on hydroelectric energy and starting to use wind, solar, and biomass energy. However, there is a source that is little used and with a capacity well above demand, which is the source of the oceans. Within this theme, the present work studies a device that generates electrical energy from the movement of oceanic or tidal currents. This equipment is called oscillating hydrofoil and is based on the oscillating movement of fish in order to operate in harmony with the environment.

Oscillating hydrofoils have been studied since 1972, with the first concept devised by Wu (1972). However, the study by McKinney and DeLaurier (1981) promoted the oscillating hydrofoil as a viable device in power generation. Other studies have emerged over the years, intending to obtain parameters that improve the device's performance.

In the published work Kinsey and Dumas (2008), several fundamental parameters for the design of an oscillating hydrofoil are analyzed, such as frequency, oscillation amplitude, efficiency, wing profiles, pivot point, and Reynolds number. As a result of this study, it was found that movement aspects have a more significant influence on performance than geometric and viscous aspects. In the work proposed by Zhu and Peng (2009), numerical simulations were performed with NACA 0005 and NACA 0025 profiles, varying aspect ratio (AR), and pivot point. Zhu and Peng (2009), obtained as a result that there is a relationship between the increase in the thickness of the profile with the production of energy for

higher frequencies.

do Prado Campos *et al.* (2021), performed an analysis for selection and mapping with eleven NACA profiles, evaluating the torque generated, in an almost static way, of each profile, at different fluid speeds. Furthermore, they found that there are significant differences between the NACA profiles in all evaluated conditions.

Within this context, the present work intends to evaluate the performance of three wing profiles under different fluid conditions (or Reynolds number). From Fig. 1, the three most used symmetric NACA profiles in the literature were selected, which are: NACA 0012, NACA 0014, and NACA 0015. The proposal is to evaluate the torque generated during the operation for each profile and check the model with the best performance for the values of Re equal to 150,000, 250,000, and 500,000.

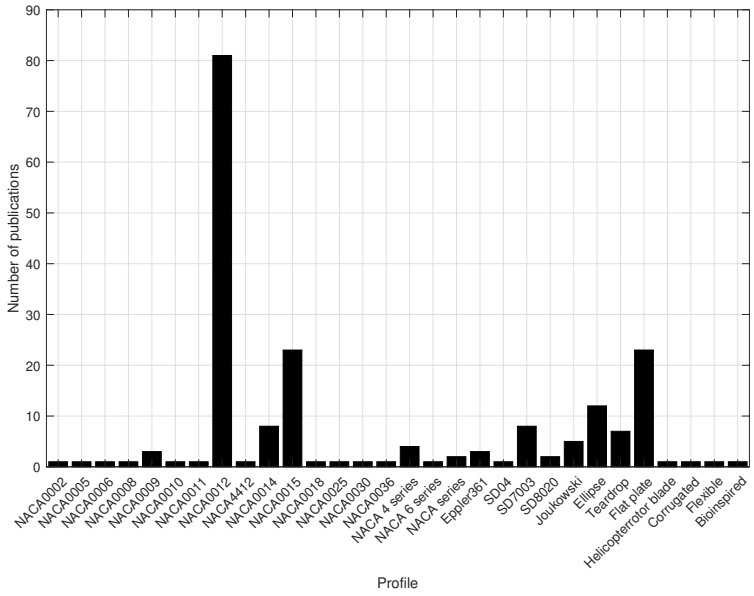

Figure 1. Profiles of the literature, adapted from do Prado Campos *et al.* (2021).

2. METHODOLOGY

Oscillating hydrofoils are influenced by viscous, geometric, and movement aspects. In the design of the dynamic model, firstly, the restrictions existing in the model of an oscillating hydrofoil are evaluated, such as limits of heave, pitch, and arm angles. In addition to the maximum angle of attack that is related to the other angles. Given these constraints and the power generation conditions, the formulations of kinematics, kinetics, and external forces that make up the equation of motion of the device are presented.

Finally, the proposed dynamic model is validated by comparing it with the results obtained by Sitorus *et al.* (2016). Thus, in Section 5, the comparison between the NACA symmetric profiles NACA 0012, NACA 0014, and NACA 0015 is performed by analyzing the forces and torques generated. The analysis is performed under three operating conditions of the fluid, with the variation of the Reynolds number.

3. DYNAMIC MODEL

In the present work, the same kinematics and kinetics proposed by do Prado Campos *et al.* (2021) were implemented in the dynamic model. However, there are significant changes with the adoption of some hydrodynamic restrictions and external forces. In this modeling, the external force is formed by the force of gravity, buoyancy and added mass, in addition to lift and drag forces. Finally, rewriting the equation of motion as a function of forces on the x and y axis.

3.1 Hydrodynamic Constraints

The oscillating hydrofoil is under the direct influence of the fluid, that is, fluid velocity, current line, type of flow, among others. Besides these, other variables can be determined in the project, such as the limit of inclination angles and operation oscillation; the maximum angle of attack; and the variable that defines whether the hydrofoil is operating in propulsion or power extraction mode.

This device is characterized by the sinusoidal movement, according to the literature Xiao and Zhu (2014). In the case of the configuration with an arm, the variable of the angle of the arm in relation to the horizontal (ψ) is added. To

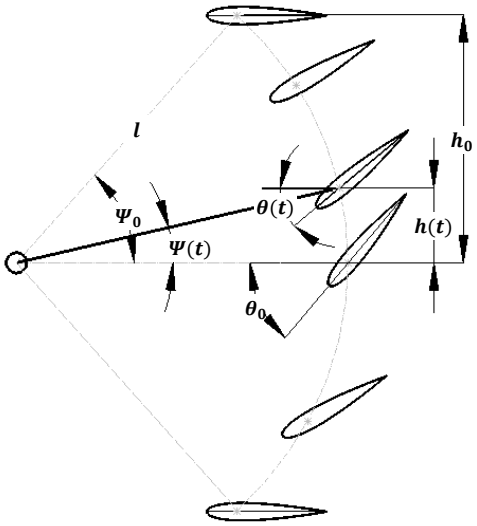

Figure 2. Angles of the hydrofoil oscillatory movement.

understand each movement, and how the variables are obtained, the formulations of each are presented through Eq.(1), Eq.(2) and Eq.(3),

$$\theta(t) = \theta_0 \cdot \sin(\omega.t) \tag{1}$$

$$h(t) = h_0 . \sin(\omega \cdot t + \phi) \tag{2}$$

$$\psi(t) = \psi_0 . \sin(\omega \cdot t + \phi) \tag{3}$$

where: θ_0 is the amplitude of the angle of *pitch*, h_0 is the amplitude of *heave*, and ψ_0 is the amplitude of the angle of the arm. ω is the frequency of movement, and ϕ is the phase.

In Figure 2, the presented variables $\theta(t)$, $h(t)$ and $\psi(t)$ are illustrated. As this is a model with arms whose length is l and can be obtained by $l = h_0/sin(\psi_0)$.

Regarding the angle of attack, according to Kinsey and Dumas (2008), in most cases, the maximum angle of attack should occur when the wing is a quarter-period of movement. Therefore, the maximum angle of attack can be written, as shown in Eq.(4),

$$\alpha_{max} = \alpha_{T/4} = \left| arctan\left(\frac{\omega \cdot h_0}{U}\right)\right| - \theta_0 \tag{4}$$

where: $\alpha_{T/4}$ is the maximum angle of attack.

According to Jones *et al.* (1997), there is a relationship to check if the wing is operating in regime of the propulsion or power extraction. Anderson *et al.* (1998) and Kinsey and Dumas (2008) also assessed the need to predict the way the device is acting. Therefore, the following formulation was proposed,

$$X = \frac{\theta_0}{arctan\left(\frac{\omega \cdot h_0}{U}\right)} \tag{5}$$

where: X is a parameter that evaluates the effect of motion on the flow regime (Kinsey and Dumas, 2008).

According to Kinsey and Dumas (2008), considering an almost stable model, for the device to be considered a propulsion device, $X < 1$ and $\alpha_{T/4} > 0$. While, for the mode power extraction $X > 1$ and $\alpha_{T/4} < 0$. In Figure 3, the expected behavior of a model with a power extraction regime is shown.

Other hydrodynamic and motion variables that are relevant for the analysis are: the relationship between the amplitude of oscillation and the chord ($h_0/\overline{c}$), the reduced frequency (f^*), the Reynolds number (Re), the wing profile model, the variation of the angle of attack, lift coefficient, drag coefficient, and pitch coefficient. In addition to the fluid characteristics, such as flow regime, flow type, fluid density, and viscosity.

3.2 External Forces

The fluid flow in the wing is capable of generating different pressure behaviors, based on changes in the angle of attack, fluid and wing characteristics, that is, as a function of the Reynolds number. The pressure generated in the wing is

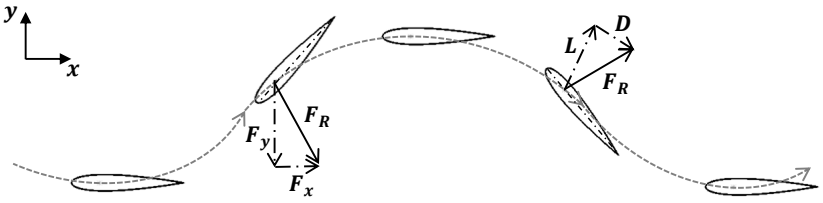

Figure 3. Energy extraction regime, $X > 1$ e $\alpha_{T/4} < 0$, adapted from Kinsey and Dumas (2008).

responsible for the hydrodynamic forces, known as drag and lift forces. In addition, the fluid is also capable of generating a buoyant force and a force due to the added mass. When this phenomenon is considered with low specific mass fluids, it does not have significant loadings and implications for the system. However, when using a fluid with a greater specific mass, this variable can be essential to bring the simulated model closer to the real one.

These forces from the fluid directly influence the dynamic behavior and, therefore, it is important to analyze different profiles. Each NACA profile studied has a different thickness, and therefore, has different behaviors of lift coefficients (C_L) and drag (C_D) for each value of Reynolds number and angle of wing attack. In this work, the data of lift, drag, and heave coefficients were used to implement XFoil in the dynamic model. On the other hand, buoyancy is a variable that depends on the volume displaced by the profile, gravity acceleration, and specific mass of the fluid, as shown by Eq. (6),

$$E = \rho \, g \, V_{perfil} \tag{6}$$

where: E is the buoyancy, ρ is the fluid's specific mass, V_p is the profile volume, and g is the gravity acceleration.

The added mass is a variable, as is the thrust, which depends on the volume of the added mass profile. However, the acceleration that acts in the formulation is the one obtained with the wing kinematics, as shown in Eq. 7,

$$F_A = \rho \, V_p \, a_{asa} \tag{7}$$

where: F_A is the force generated by the added mass, ρ is the fluid's specific mass, V_p is the profile volume, and a_{wing} is the wing acceleration.

In the analysis of the resulting forces, the variables are separated, placing them in Cartesian coordinates (x, y), as discussed in the literature Kinsey and Dumas (2008); Simpson (2009); Truong *et al.* (2014). Thus, the force in the x direction can be written as,

$$F_x = L.sin(\gamma) - D.cos(\gamma) \tag{8}$$

where: L is the lift force ($L = 1/2 \cdot \rho \cdot A_p \cdot C_L \cdot U^2$) and D is the drag force ($D = 1/2 \cdot \rho \cdot A_p \cdot C_D \cdot U^2$), where A_p is the projected area of the profile and U is the fluid velocity.

In Equation (9), the force in the y direction is presented, being presented in Figure 4, the resulting components of the forces.

$$F_y = L.cos(\gamma) + D.sin(\gamma) - F_g + E + F_A \tag{9}$$

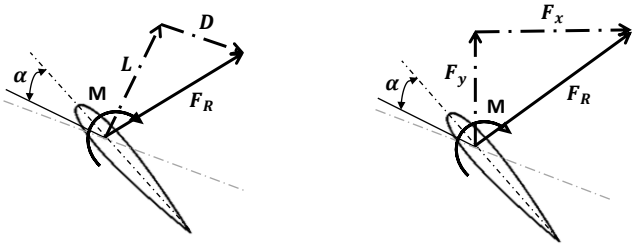

(a) (b)

Figure 4. Wing forces: (a) Hydrodynamic forces e (b) Components of result force.

The application of these variables in the dynamic model is made through the external torque, called hydrodynamic torque. Thus, the cross product between the position vector and the vector of the hydrodynamic efforts was considered, as shown in the cross product of Eq.(10),

$$\tau_{ext} =^0 P_{g2}.F_R + M_{c/4} \tag{10}$$

Table 1. Oscillating hydrofoil specifications for validation

Parameters	Values	Parameters	Values
Fluid	Water	Wing Profile	NACA 0012
Especific mass (ρ)	$997.13\ kg/m^3$	Chord length	$0.15\ m$
Kinematic viscosity (ν)	$9.95 \times 10^{-7}\ m^2/s$	Span length	$0.29\ m$
Arm length	$0.185\ m$	Profile Area	$0.0435\ m^2$
Arm mass	$0.267\ kg$	Pivot point	$0.25.\overline{c}$
Wing mass	$0.1825\ kg$	Gearbox moment of inertia	$0.0069\ kg\ m^2$
Moment of inertia	$0.0093\ kg\ m^2$	Damping coefficient	$0.45\ N\ m\ s$

where: τ_{ext} is the external torque generated by the hydrodynamic forces, ${}^0P_{g2}$ is the wing position vector in relation to the inertial frame, F_R is the force resulting from the forces (F_y and F_x), while $M_{c/4}$ is the pitch moment. This definition allows direct application to the equation of motion discussed below.

3.3 Motion Equation

The device's equation of motion can be obtained through kinematics, dynamics, and hydrodynamic efforts. However, depending on the analysis, the proposed oscillating hydrofoil model was simplified to 1-DOF. With this, the equation of motion Eq.(11) can be rewritten,

$$\ddot{q} = M^{-1}[({}^0P_{g2x} \cdot F_y - {}^0\ P_{g2y} \cdot F_x) + M_{c/4} - H - G - Di] \tag{11}$$

where: M is relates mass-inertia matrix , H is the Coriolis effect, centrifugal and gyroscopic forces, G is gravity and Di is dissipative effects.

4. MODEL VALIDATION

The mathematical modeling of the device was implemented in Matlab© software, and simulations were performed to compare the proposed model with the Truong *et al.* (2014) and Sitorus *et al.* (2016) model.

In the works of Truong *et al.* (2014) and Sitorus *et al.* (2016), the same experimental apparatus were used whose fluid data, constructive and operational specifications of the oscillating hydrofoil, can be seen in Table 1. Furthermore, in the proposed model, the values of lift coefficient (C_L) and drag (C_D) were used, close to the values used by Truong *et al.* (2014). The data for C_L and C_D were obtained through the work done by Sheldahl and Klimas (1981), with $Re = 0.86 \times 10^5$ for the profile NACA 0012. As well as the values of the moment coefficients (C_M).

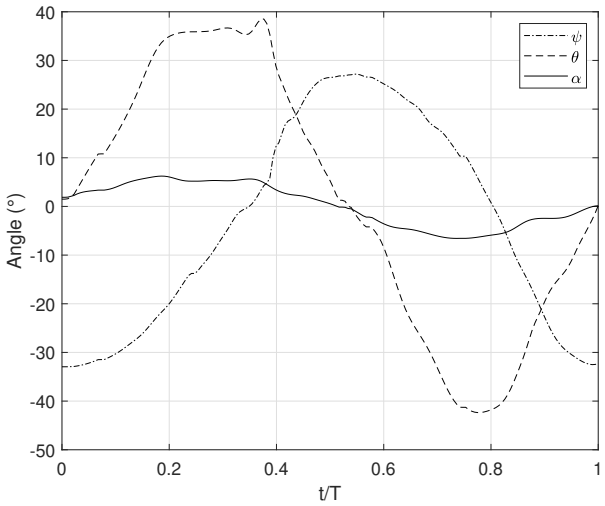

Figure 5. Angles of attack, inclination and arm, considering NACA 0012, θ varies between $37.5°$ and $-39.8°$; ψ ranges between $27.0°$ and $-33.4°$; $f^* = 0.157$; $h_0/\overline{c} = 0.748$.

The model proposed by Sitorus *et al.* (2016) is a passive device; that is, it does not have the action of an actuator on the wing. Thus, the movement is induced by the fluid and can present any movement. When observing the graphs of angles

Table 2. Simulation parameters.

Parameters	Values	Parameters	Values
Fluid	Water	Wing Profiles	NACA 0012, 0014 and 0015
Especific mass (ρ)	$999\ kg/m^3$	Chord length	$0.24\ m$
Kinematic viscosity (ν)	$9.79 \times 10^{-7}\ m^2/s$	Span length	$1.68\ m$
Arm length	$0.709\ m$	Reduced frequency (f^*)	0.08
Arm mass	$12.16\ kg$	Pivot point	$0.25.\overline{c}$
Wing mass	$18.49\ kg$	Ratio heave-chord ($h_0/\overline{c}$)	1.5
Moment of inertia	$0.3517\ kg\ m^2$	Damping coefficient	$0.2\ N\ m\ s$
Tilt range (θ_0)	60°	Maximum attack angle (α_{max})	22°

obtained by Sitorus *et al.* (2016), it is clear that there are cases whose behavior is similar to a sinusoidal function. As a result, in the other sections, sinusoidal functions are used to represent the system's kinematics.

In the model validation, the same angle curves obtained by Sitorus *et al.* (2016) were used, as can be seen in Figure 5. In this Figure, the results of the angles of movement of the arm and wing are presented, in addition to the angle of attack.

In Figure 6, the results of the force resulting from the coordinate y (F_y) of the proposed model are presented, compared with the values obtained by Sitorus *et al.* (2016) through simulation CFD and analytically. In Figure 6, the results regarding the force resulting from the coordinate x (F_x) are presented, and the same comparison is performed.

By analyzing Figure 6, it is clear that the behavior obtained by the proposed model is similar to the model of Sitorus *et al.* (2016). However, there is a difference between the values in the first (positive) peak of the force Y, which occurred because the same lift and drag coefficient values were not used. Besides, the speeds were also a little different. At the second (negative) peak, the maximum values and curve behavior are similar.

In the case of F_x, the difference occurs at both peaks. This is for the same reasons discussed for F_y. However, the behavior of the curves is similar, even with the second peak being larger than the first.

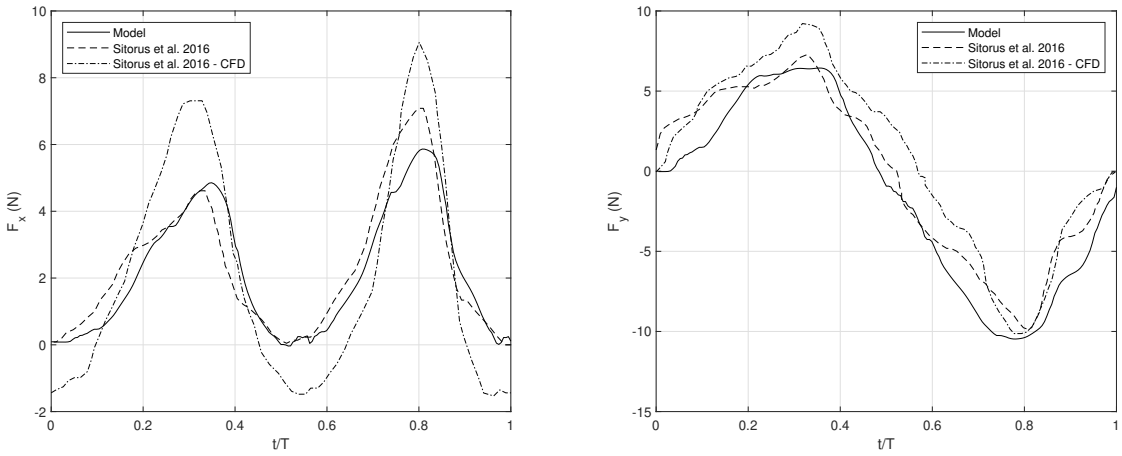

Figure 6. Result force in the axis X and Y, considering NACA 0012, θ varies between 37.5° and -39.8°; ψ ranges between 27.0° and -33.4°; $f^* = 0.157$; $h_0/\overline{c} = 0.748$.

5. RESULTS AND DISCUSSIONS

The structure of the device used in the analysis is similar to that conceived by Campos *et al.* (2019). However, the profile models and device movement are different. In the present work, three symmetric NACA profiles, NACA 0012, NACA 0014, and NACA 0015, are simulated under the same operating conditions. In addition, the Reynolds number variation is performed, in order to assess which profile is more suitable in each situation.

The movement aspects are the same in the three Reynolds number cases. The angle of pitch, heave, angle of arm, and angle of attack have the same behavior in all cases, as shown in Fig. 7. As for the geometric aspects, the length of the chord, span, and arm are constant, and the only change is the NACA profile, that is, the thickness of the profile. Finally, in the viscous aspect, the flow is considered laminar. The reduced frequency is constant and with a value that allows considering an almost stable system in a steady state. In Table 2, the constant geometric and viscous parameters are displayed.

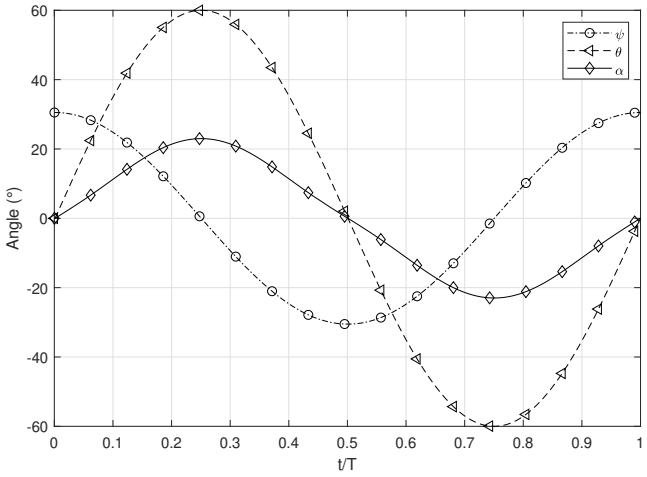

Figure 7. Angles of arm, pitch and angle of attack during a cycle.

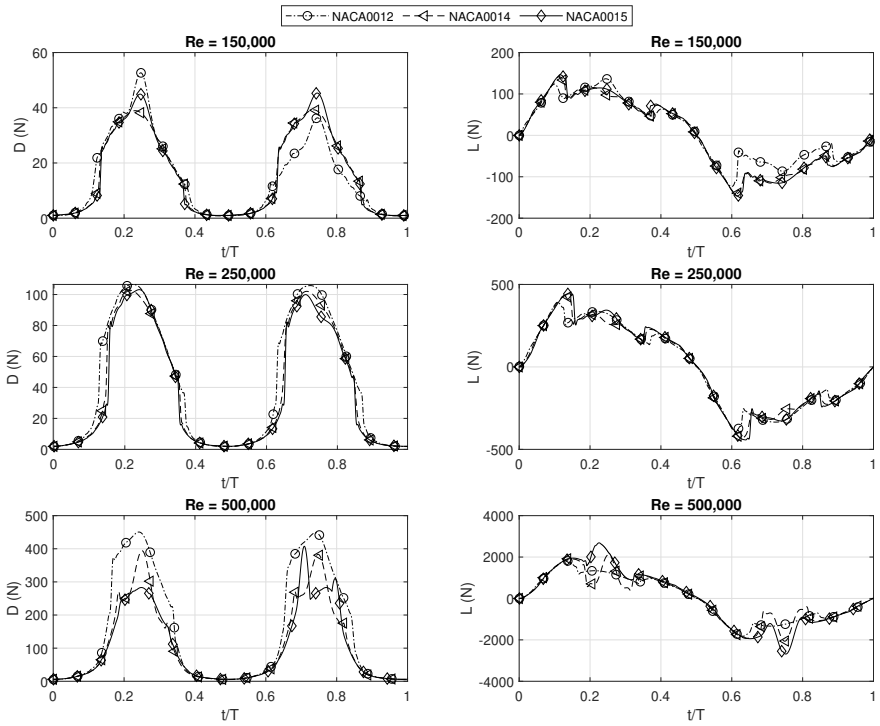

Figure 8. Lift and Drag forces during a cycle, considering NACA 0012, NACA 0014 and NACA 0015, Re ranging between 1.5×10^5 and 5.0×10^5.

In the analysis of the profiles, the behavior of the lift and drag forces was first verified. In Figure 8, the three profiles (NACA 0012, NACA 0014 and NACA 0015) in the three operating situations are presented. It is important to highlight that everyone had the expected behavior. However, in the case of drag force, in all cases the NACA 0012 presented the highest values, which resulted in low performance. With respect to lift force, in operations with Reynolds number equal to 1.5×10^5 and 2.5×10^5, there is a drop in lift due to wing stall, between time 0.15 and 0.38, the same occurs between the instant 0.61 and 0.84. In the case of Re= 5.0×10^5, the behavior is different, with peaks at the point of greatest angle of attack.

Another analysis performed was the comparison between the resulting forces (F_x and F_y) obtained by each profile, in each operation situation. In Figure 9, the same cases seen in Figure 8 were presented, and the behaviors were also similar. Note that there are moments of oscillation of some profiles that may be due to uncertainties in the data collected from the panel methods used in the XFoil algorithm.

In Figure 10, the behavior of the torques of each profile along an operating cycle is presented. In the cases of Re =

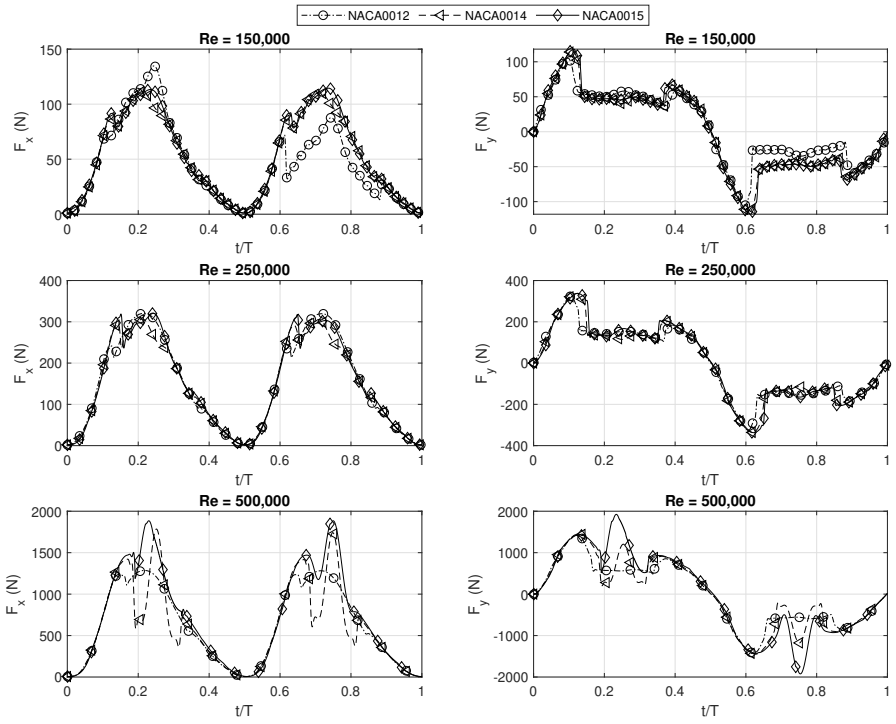

Figure 9. Component X an Y of result force during a cycle, considering NACA 0012, NACA 0014 and NACA 0015, Re ranging between 1.5×10^5 to 5.0×10^5.

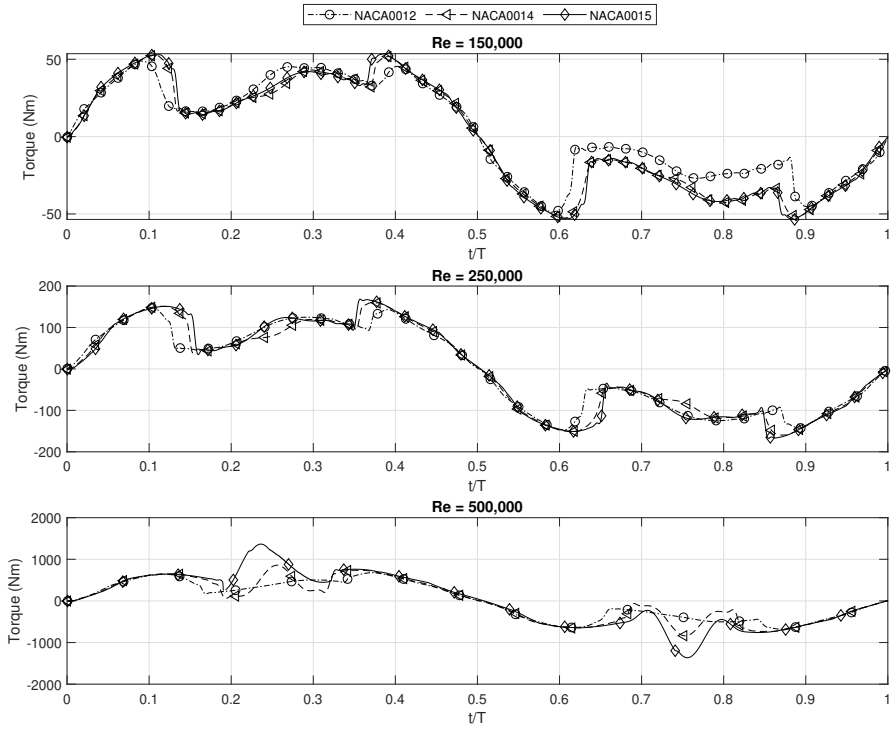

Figure 10. Torque curve during a cycle, considering NACA 0012, NACA 0014 and NACA 0015, Re ranging between 1.5×10^5 and 5.0×10^5.

1.5×10^5 and Re = 2.5×10^5, it is observed that the three profiles have the same behavior, with the NACA 0014 and NACA 0015 profiles having outstanding values. Close throughout the cycle, while the NACA 0012 profile performs worse than the other ones. In the case of Re = 5.0×10^5, there is a difference in behavior that may be related to changes in the values

Table 3. Potência média do gerador durante a operação.

Torques	NACA 0012	NACA 0014	NACA 0015
$T_{max}^{Re1.5}$ (Nm)	48.9	52.8	53.6
$T_{m}^{Re1.5}$ (Nm)	27.3	31.6	32.4
$T_{q}^{Re1.5}$ (Nm)	30.2	34.2	35.1
$T_{max}^{Re2.5}$ (Nm)	147.5	159.8	168.3
$T_{m}^{Re2.5}$ (Nm)	91.1	94.3	98.6
$T_{q}^{Re2.5}$ (Nm)	98.5	103.1	107.8
$T_{max}^{Re5.0}$ (Nm)	678.5	858.0	1364.9
$T_{m}^{Re5.0}$ (Nm)	400.0	436.6	548.3
$T_{q}^{Re5.0}$ (Nm)	438.9	494.2	625.2

of lift and drag coefficients due to the maximum angle of attack. Finally, in Table 3, the maximum (T_{max}), mean (T_m) and quadratic torque (T_q) of each profile in each operating situation are presented. In all cases, the NACA 0015 presented the best result, however for a lower Reynolds number (1.5×10^5), the NACA 0015 and NACA 0014 values were close.

6. CONCLUSION

The present work analyzed three symmetric NACA profiles (NACA 0012, NACA 0014, and NACA 0015) in similar operating situations, modifying only the Reynolds number. This study found that in the case of Reynolds number equal to Re = 1.5×10^5, the profiles NACA 0014 and NACA 0015 generates similar torque, while in the cases of Re = 2.5×10^5 and Re = 5.0×10^5, the NACA profile NACA 0015 is the most suitable.

The proposed analysis presented satisfactory results, but has some parts that could be improved. A limited parameter in the proposed study was the angle of attack, which operated up to the maximum value of 22 ^{circ}, this due to the data extracted from XFoil being unstable from the above values. In future works, experimental analyzes or simulations in CFD (Computational Fluid Dynamics) are suggested, which use the RANS approach, collecting more accurate data after the wing stall.

7. REFERENCES

Anderson, J.M., Streitlien, K., Barrett, D. and Triantafyllou, M.S., 1998. "Oscillating foils of high propulsive efficiency". *Journal of Fluid mechanics*, Vol. 360, pp. 41–72.

Campos, G.A.P., Raptopoulos, L.S.C. and Dutra, M.S., 2019. "Mathematical model for flapping foil". In *Proceedings of the 25nd International Congress of Mechanical Engineering - COBEM 2019*. Uberlândia, Brazil.

do Prado Campos, G.A., Raptopoulos, L.S.C. and Dutra, M.S., 2021. "Mapping and selection of profiles for morphing wing of a flapping foil". *Journal of the Brazilian Society of Mechanical Sciences and Engineering*, Vol. 43, p. 73.

Jones, K., Platzer, M., Jones, K. and Platzer, M., 1997. "Numerical computation of flapping-wing propulsion and power extraction". In *35th Aerospace Sciences Meeting and Exhibit*. p. 826.

Kinsey, T. and Dumas, G., 2008. "Parametric study of an oscillating airfoil in a power-extraction regime". *AIAA journal*, Vol. 46, No. 6, pp. 1318–1330.

McKinney, W. and DeLaurier, J., 1981. "Wingmill: an oscillating-wing windmill". *Journal of energy*, Vol. 5, No. 2, pp. 109–115.

Sheldahl, R.E. and Klimas, P.C., 1981. "Aerodynamic characteristics of seven symmetrical airfoil sections through 180-degree angle of attack for use in aerodynamic analysis of vertical axis wind turbines". Technical report, Sandia National Labs., Albuquerque, NM (USA).

Simpson, B.J., 2009. *Experimental studies of flapping foils for energy extraction*. Ph.D. thesis, Massachusetts Institute of Technology.

Sitorus, P.E., Le, T.Q., Ko, J.H., Truong, T.Q. and Park, H.C., 2016. "Design, implementation, and power estimation of a

lab-scale flapping-type turbine". *Journal of Marine Science and Technology*, Vol. 21, No. 1, pp. 115–128.

Truong, T., Sitorus, P.E., Park, H., Tambunan, I., Putra, H., Ko, J. and Kang, T., 2014. "Nonlinear dynamic model for flapping-type tidal energy harvester". *Journal of Marine Science and Technology*, Vol. 19, No. 4, pp. 406–414.

Wu, T., 1972. "Extraction of flow energy by a wing oscillating in waves". *Journal of Ship Research*, Vol. 16, pp. 66–78.

Xiao, Q. and Zhu, Q., 2014. "A review on flow energy harvesters based on flapping foils". *Journal of fluids and structures*, Vol. 46, pp. 174–191.

Zhu, Q. and Peng, Z., 2009. "Mode coupling and flow energy harvesting by a flapping foil". *Physics of Fluids*, Vol. 21, No. 3, p. 033601.

8. RESPONSIBILITY NOTICE

The following text, properly adapted to the number of authors, must be included in the last section of the paper: The author(s) is (are) solely responsible for the printed material included in this paper.